Cell Transplantation, Vol. 24, pp. 1451–1467, 2015
Printed in the USA.

0963-6897/15 $90.00 + .00
DOI: http://dx.doi.org/10.3727/096368914X683034
E-ISSN 1555-3892
www.cognizantcommunication.com

Electrophysiological Characterization of eGFP-Labeled Intrastriatal Dopamine Grafts

Meltem Hohmann,*† Regina Rumpel,* Martin Fischer,‡ Malte Donert,* Andreas Ratzka,* Alexander Klein,* Maike Wesemann,* Anna Effenberg,* Christoph Fahlke,§ and Claudia Grothe*†

*Institute of Neuroanatomy, Hannover Medical School, Hannover, Germany
†Center for Systems Neuroscience, Hannover, Germany
‡Institute of Neurophysiology, Hannover Medical School, Hannover, Germany
§Institute of Complex Systems, Zelluläre Biophysik, FZ Jülich, Jülich, Germany

Substitution of degenerated dopaminergic (DA) neurons by intrastriatally transplanted ventral mesencephalon (VM)-derived progenitor cells has been shown to improve motor functions in parkinsonian patients and animal models, whereas investigations of electrophysiological properties of the grafted DA neurons have been rarely performed. Here we show electrophysiological properties of grafted VM progenitor cells at different time intervals up to 12 weeks after transplantation measured in acute brain slices using eGFP-Flag transfection to identify the graft. We were able to classify typical DA neurons according to the biphasic progression (voltage "sag") to hyperpolarizing current injections. Two types of DA-like neurons were classified. Whereas type 1 neurons were characterized by delayed action potentials after hyperpolarization and irregular spontaneous firing, type 2 neurons displayed burst firing after hyperpolarization, spontaneous bursts, and regular firing. Comparison to identified DA neurons in vitro indicates a high integration of the intrastriatally grafted neurons, since in vitro cultures displayed regular firing spontaneously, whereas grafted identified DA neurons showed irregular firing. Additionally, type 1 and type 2 neurons exhibited a slight increase in the spontaneous firing frequency over time intervals after grafting, which might reflect a progressive integration of the grafted DA neurons. Our results provide evidence of the differentiation of grafted VM progenitor cells into mature integrated DA neurons, which are shown to replace the missing DA neurons functionally early after grafting.

Key words: Parkinson's disease (PD); Dopaminergic (DA) neurons; Cell replacement; Patch clamp technique; Enhanced green fluorescent protein (eGFP) transfection

INTRODUCTION

Parkinson's disease (PD) is characterized by a severe loss of dopaminergic (DA) neurons in the substantia nigra pars compacta (SNpc), resulting in movement disorders like tremor, akinesia, bradykinesia, and rigor. Cell replacement represents a possibility to substitute the degenerating DA system. Although intrastriatally transplanted embryonic cells of the ventral mesencephalon (VM) revealed improved motor functions of PD patients in clinical trials (10,23), side effects like graft-induced dyskinesia (30) and limited availability of donor tissue (1,46) require further investigations. Analyses of the electrophysiological properties of transplanted cells could have an impact on the improvement of cell replacement strategies. So far, there are only few data on the electrophysiological characteristics of intrastriatal grafts in the rat model of PD (9,39,43), whereas electrophysiological properties of DA neurons within the SNpc have been extensively investigated. DA neurons are pacemaker neurons. They are characterized by wide action potential durations, prominent afterhyperpolarization amplitudes, and spontaneous regular firing at low frequencies (7,15,34,35). Pacemaker neurons occur in the heart, retina, and motor system. A prominent typical property of pacemaker neurons is the hyperpolarization-induced inward current (31). Hyperpolarization-activated cyclic nucleotide-gated (HCN) channels regulate the generation of repetitive firing (44). Regarding the target of DA neurons of the SNpc, the striatum, DA denervation induces an increased spontaneous activity of striatal neurons as well as an increased firing rate, which, notably, can be normalized after intrastriatal grafting of VM-derived cells (7). Interestingly, DA deficiency in the striatum also induces an increased firing rate and burst activity in the subthalamic nucleus, which can be partially normalized after

Received February 14, 2014; final acceptance July 11, 2014. Online prepub date: July 15, 2014.
Address correspondence to Prof. Dr. C. Grothe, Hannover Medical School, Institute of Neuroanatomy (OE4140), Carl-Neuberg-Strasse 1, 30625 Hannover, Germany. Tel: +49 511 532-2897; Fax: +49 511 532-2880; E-mail: grothe.claudia@mh-hannover.de

intrastriatal DA cell transplantation in hemiparkinsonian rats (36). Moreover, as recently shown, VM grafts restore long-term synaptic plasticity in the host striatum regions, which were densely innervated by DA neurons (37). Up to now, different approaches were followed to electrophysiologically evaluate intrastriatally transplanted DA neurons. Fisher and coworkers performed "blind" extracellular recordings via four additional holes in the skull and showed that after intrastriatal transplantation, DA neurons fire in an irregular or a bursting manner (9), whereas DA neurons in vitro were mainly silent (20). This might be due to the missing input from the striatum, although spontaneous activity of DA neurons is shown to be self-generated (13,21). Sørensen and coworkers transplanted genetically labeled mouse VM cells into intact or DA-lesioned striata of neonatal rats and measured the functional integration of labeled DA neurons using brain slices (39).

In the present study, functional characteristics and synaptic integration were evaluated in VM-derived progenitor cells after intrastriatal transplantation into the adult striatum in the unilateral 6-hydroxydopamine (6-OHDA) rat model of PD in situ. The transfection of rat embryo-derived VM progenitor cells expressing enhanced green fluorescent protein (eGFP) enabled the visualization/identification of the grafts even 12 weeks after transplantation. The bipolar membrane potential generated by the hyperpolarization-activated inward current of DA neurons was utilized to distinguish between grafted DA and non-DA neurons. In addition, DA neurons derived from transgenic mice expressing GFP under the control of the tyrosine hydroxylase (TH)-promotor were directly recorded in vitro and in situ after xenotransplantation into the adult rat PD model and were compared with the collected electrophysiological properties of the grafted rat progenitor cells.

MATERIALS AND METHODS

Animals

Female Sprague–Dawley (SD) rats obtained from Charles River (Sulzfeld, Germany) and female transgenic tg (TH-GFP)$^{6\text{-}7\text{Koba}}$ mice on C57BL/6 genetic background (38) were kept with ad libitum access to food and water. All experimental protocols followed the German law on animal care and were approved by the Bezirksregierung LAVES (Hannover, Germany).

Experimental Design

Three sets of experiments were performed (Fig. 1): i) eGFP-Flag-transfected rat VM-derived progenitor cells were intrastriatally transplanted into the adult rat 6-OH DA-lesioned PD model; grafted cells were electrophysiologically recorded in brain slice preparations at different time intervals for up to 12 weeks after transplantation. ii) VM-derived dissociated cell cultures of TH-GFP transgenic mice were characterized immunocytochemically (ICC), and DA neurons were electrophysiologically recorded. iii) VM-derived cell suspensions of TH-GFP transgenic mice were intrastriatally transplanted into the adult rat 6-OHDA-lesioned PD model; grafted cells were electrophysiologically recorded in brain slice preparations 6 weeks after transplantation. Measurements of the different approaches were compared and enabled a characterization of the grafted rat progenitor cells.

Preparation of VM Primary Cell Suspension

Primary cultures of DA progenitor cells were prepared from dissociated cell suspensions of the dissected VM on embryonic day (E) 12 (SD-rats) (Fig. 1, exp. i), E13 (TH-GFP mice; for transplantation) (Fig. 1, exp. iii), and E14 (TH-GFP mice; in vitro patch clamp experiment) (Fig. 1, ii). Transgenic green fluorescent embryos derived from crosses of hemizygous TH-GFP male mice with wild-type TH-GFP female mice were selected under visual control (fluorescence microscope; Leica Microsystems, Wetzlar, Germany) and subsequently used to isolate the VM.

Dissection and dissociation of the fetal rat VM was previously described in detail (33). Briefly, VMs were incubated in preparation medium that consisted of 1 mM sodium pyruvate (PAA, Cölbe, Germany), 2 mM L-glutamine (PAA), 1×B27 (Gibco, Darmstadt, Germany), and 0.05% DNAse (Roche, Mannheim, Germany) for 15 min at 37°C. After adding adhesion medium [SD rats: Dulbecco's modified Eagle's medium/Ham's F-12 medium (DMEM/F12; Gibco) containing 3% fetal calf serum (FCS; PAA), 1×N2 (Gibco), 1 mM sodium pyruvate (PAA), 0.25% bovine serum albumin (BSA; PAA), 2 mM L-glutamine (PAA), 20 ng/ml fibroblast growth factor-2 (FGF-2; Peprotech, Hamburg, Germany), and 1×B27 (Gibco); TH-GFP mice: DMEM/F12 (Gibco) containing 5% FCS (PAA), 1×N2 (Gibco), 1 mM sodium pyruvate (PAA), 0.25% BSA (PAA), 2 mM L-glutamine (PAA)], cells were centrifuged at 235×*g* for 5 min. Cells were resolved and dissociated mechanically in adhesion medium using Eppendorf pipettes (2,33). The concentration of the cells was estimated by using the trypan blue exclusion assay system (Sigma-Aldrich, Steinheim, Germany).

Cell Culture

E12 SD rat VM cell suspensions were used in experiment i (Fig. 1). Dissociated VM progenitor cells were seeded first in an amount of 600,000 cells per well in the proliferation plate (Nunc 6-well multidish; Thermo Scientific, Rockford, IL, USA) to reach high numbers for transfection and second in an amount of 400,000 cells per well that served as a bottom layer for transfected cells. After 1 day of adhesion and 3 days of proliferation [similar composition to the adhesion medium without FCS (PAA) and B27 (Gibco)], the cells of the proliferation

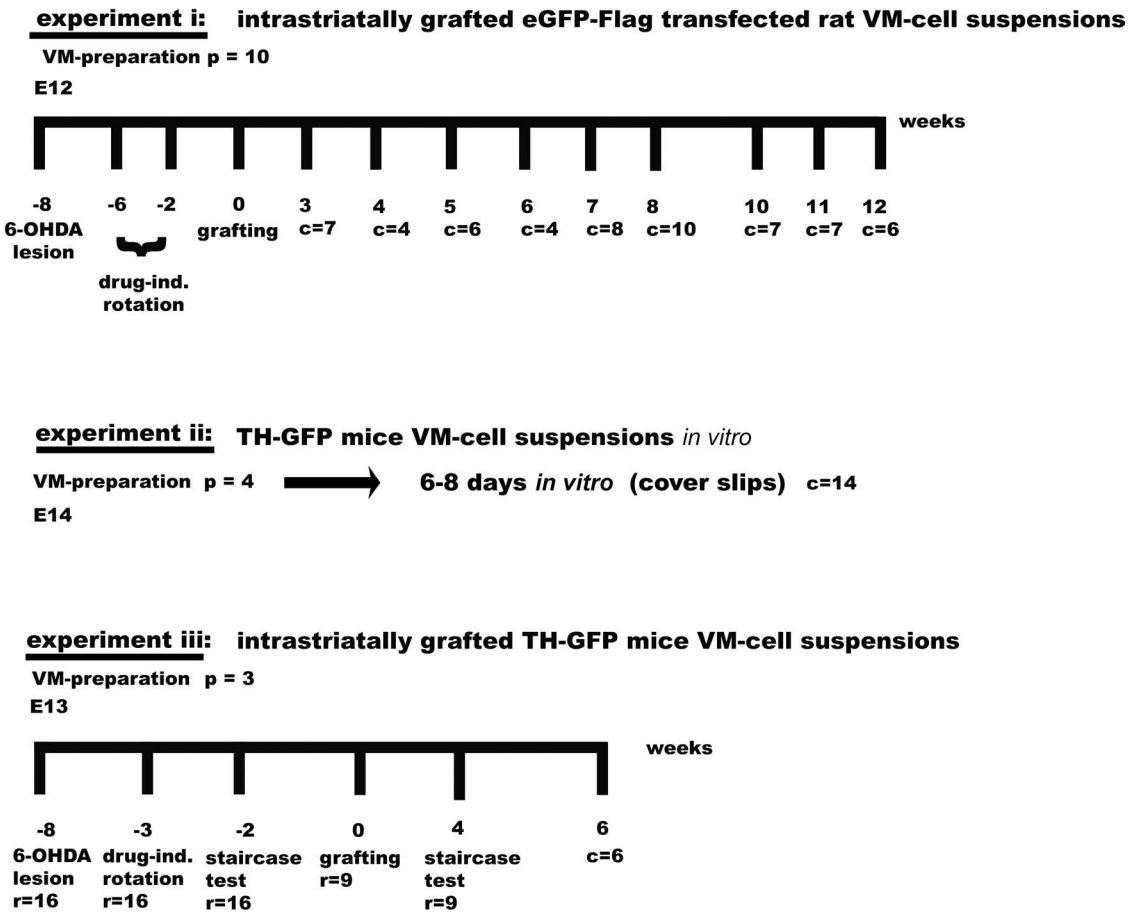

Figure 1. Overview of the experimental design. (i) Ten grafting sessions were performed with eGFP-Flag-transfected VM cell suspensions derived from rat embryos. Whole-cell patch clamp recordings were performed 3 to 12 weeks after grafting. Recorded slices were stained against TH and biocytin. (i, iii) Additionally, whole-cell recordings of genetically labeled dopaminergic neurons derived from TH-GFP mice embryos were performed in VM cell cultures in vitro [6 to 8 days in vitro (DIV), ii] and 6 weeks after intrastriatal grafting in acute brain slices (iii). Grafts and VM cultures were stained with TH-antibody. p, preparations; r, grafted rats; c, recorded cells.

plate were detached. Two million cells were resuspended in 100 µl nucleofection solution (Amaxa basic nucleofector kit–primary neurons; Lonza, Basel, Switzerland) and transfected with an eGFP-expressing plasmid [5 µg pCAGGS-EGFP-Flag plasmid described in (33)] using the nucleofector program A-033 (4,33). The transfected cells were seeded in a ratio of 1:3 on top of the bottom layer cultures of the second well. The colayer culture protocol enables high transfection efficiencies while keeping high numbers of DA neurons from the bottom layer of the undetached and nontransfected cells (33). After 2 days of differentiation [DMEM/F12 containing 1% FCS (PAA), 0.25% BSA (Sigma-Aldrich), 2 mM L-glutamine (PAA), 1× B27 (Gibco), and 100 µM L-ascorbic acid (Sigma-Aldrich)], the cells of the colayer were detached and transplanted into the lesioned rat striatum as described previously (33). Ten preparations/transfections were performed for transplantation. Transplanted rats ($n=31$) were evaluated at different time points (Fig. 1, exp. i).

For whole-cell patch clamp experiments, five TH-GFP mouse VM preparations (E14) were performed (Fig. 1, exp. ii). Dissociated cell cultures were seeded in a concentration of 100,000–300,000 cells per well on polyornithine (0.6 mg/ml; Sigma-Aldrich)/laminin (6 µg/ml; BD Biosciences, Bedford, MA, USA)-coated coverslips in 24-well plates. After adhesion in neurobasal medium [DMEM/F12 (Gibco), 5% FCS (PAA), 1 mM sodium pyruvate (PAA), 0.25% BSA (PAA), 2 mM L-glutamine (PAA), N2 (Gibco), and 5% FCS (PAA)] overnight, cells were differentiated for 5 to 8 days in neurobasal medium containing 50 µg/ml recombinant high molecular weight (HMW) FGF-2 (prepared by Dr. P. Claus, Neuroanatomy, Hannover Medical School). Differentiated cells were either fixed for ICC examination of the DA neurons or were used for whole-cell patch clamp experiments. For recording experiments, the differentiation medium was replaced by artificial cerebrospinal fluid (ACSF) that consisted of 125 mM NaCl (J.T. Baker, Deventer, Holland), 25 mM

$NaHCO_3$ (Merck, Darmstadt, Germany), 2.5 mM KCl_2 (Merck), 1.25 M NaH_2PO_4 (Fluka, Steinheim, Germany), 2 mM $CaCl_2$ (Sigma-Aldrich), 1 mM $MgCl_2$ (J.T. Baker), 25 mM glucose (Sigma-Aldrich), and 10 mM HEPES (SERVA Electrophoreses GmbH, Heidelberg, Germany). Fluorescent neurons were chosen by fluorescence microscopy (Leica DM LFSA) and recorded under transmitted light. The neurons of a single coverslip were recorded for up to 1.5 h.

For transplantation of primary TH-GFP mice cell suspensions, VM preparations of the slightly younger stage E13 were used to achieve a better integration into the host tissue (Fig. 1, exp. iii). The GFP-expressing embryos were selected by fluorescence microscopy. The dissected VM tissues were collected and stored for 1 to 3 days in B27 (2×)-supplemented hibernation medium (hibernate-E CTS, Gibco) at 4°C (3,28). Hibernation was performed to have sufficient donor tissue on the day of transplantation, as time mating was performed at three consecutive days using six female mice. The collected GFP-expressing VM tissues were incubated for 15 min at 37°C in DMEM containing trypsin (0.025%, Gibco) and DNAse (0.05%, Roche). Afterward, tissue was washed four times with DMEM/F12 containing DNAse (0.05%) following centrifugation at 235 × *g* for 5 min. The tissue was resolved and dissociated into a single cell suspension containing 130,000 cells/µl. Nine 6-OHDA-lesioned rats were intrastriatally grafted.

6-OHDA Lesion and VM Cell Suspension Transplantation

A 6-OHDA lesion was performed according to a previous protocol (33). In brief, rats were anesthetized with chloral hydrate (370 mg/kg body weight, IP; Sigma-Aldrich). Animals received one stereotaxic injection of 6-OHDA hydrobromide (free base 5.14 µg/µl in 0.03% L-ascorbate-saline; Tocris, Briston, UK) into the right medial forebrain bundle using a 10-µl Hamilton syringe (Hamilton, Bonaduz, Switzerland) with an injection rate of 1 µl/min. The following coordinates in millimeters according to bregma and dura (32) were used: anterior–posterior (AP) −4.0, lateral (LAT) −1.3, dorsoventral (DV) −7.0, and tooth bar (TB) −4.5 with an injection volume of 3 µl (42). The cannula was left in place for an additional 2 min to allow diffusion before being slowly retracted.

Rats were selected for transplantation according to the lesion success estimated in the drug-induced rotation test and the paw preference of the staircase test. Intrastriatal transplantations of TH-GFP mice cell suspensions and SD rat cell suspensions were performed with 130,000 cells/µl by two stereotactic injections [two tracts, four deposits of 1 µl cell suspension each into the right striatum using a glass capillary (Drummond Scientific, Gauting, Germany)] at the following coordinates (in mm according to bregma and dura): medial tract, AP +0.5, LAT −2.3, DV −5, and −4, TB 0.0; lateral tract, AP +0.5, LAT −3.3, DV −5, and −4, TB 0.0 (33,41). Rats that were grafted with TH-GFP mouse progenitor cells were injected with cyclosporine (1 mg/100 g body weight, IP; Novartis, Nürnberg, Germany). Treatment was started 1 day in advance and continued daily after grafting.

Drug-Induced Rotation Test

Six weeks after 6-OHDA lesion, rats were monitored in automatic rotometer bowls. As previously described, animals were injected with 0.05 mg/kg body weight L-apomorphine hydrochloride (Sigma-Aldrich) in ascorbate-saline and 3 days later with 2.5 mg/kg body weight D-amphetamine sulfate (Sigma-Aldrich) in saline. Right and left full turns were automatically counted for 40 min (apomorphine) and 90 min (amphetamine) (33). Animals were considered fully lesioned when they demonstrated at least four turns per minute contralaterally after apomorphine injection and six turns per minute ipsilaterally after amphetamine injection.

Staircase Test

Motor skills of lesioned rats were additionally investigated by a paw-reaching test (8,26,29). All tested animals were food deprived (reduced to 12 g standard food pellet per animal per day) during the period of the testing days and 1 day in advance. The body weight was controlled every second day ensuring a maintenance of at least 80% of the pretest body weight. Rats were placed into the staircase boxes for 5–10 min to habituate to the surroundings for the first 4 days. On the third and fourth day of habituation, pellets were distributed where they were easily accessible inside the box. The actual experiment started on day 5. The test was performed for 15 min per run on 11 following days. Each of the seven stairs was loaded with four sugar pellets. The total amount of pellets reached, eaten, and the maximal distance within every run was estimated for each animal's left and right paw separately. In the second session, the test was repeated with the grafted animals 5 weeks after transplantation. The number of eaten pellets and the maximal reached distance by the right and left paw of each animal on the last 5 days was averaged. Statistical analysis was performed using one-way ANOVA and Tukey's multiple comparisons test comparing the skills of the ipsilateral (right) and contralateral (left) paw after lesion with the skills after transplantation (GraphPad PRISM 6; GraphPad Software, San Diego, CA, USA). Statistical significance was set at $*p<0.05$, $**p<0.01$, $***p<0.001$.

Immunohistochemistry (IHC) and Immunocytochemistry (ICC)

The recorded brain slices were fixed in 4% paraformaldehyde (PFA; Sigma-Aldrich) in Dulbecco's phosphate-buffered saline (PBS; Biochrom, Berlin, Germany)

overnight at 4°C. Primary cultures of TH-GFP neurons were fixed in 4% PFA in PBS for 15 min.

After preincubation [0.3% Triton-X-100 (Roche), 3% normal goat serum (NGS; Gibco) in PBS], slices and cell cultures, respectively, were incubated with the first antibody anti-TH (AB152, 1:500; Millipore, Ternecula, CA, USA) with 0.3% Triton X-100 (Roche) and 3% NGS (Gibco) in PBS at 4°C overnight. The secondary antibody anti-rabbit Alexa 647/555 (A-21247/A-210042, 1:500; Molecular Probes, Karlsruhe, Germany) with 0.3% Triton X-100 (Roche) and 1% NGS (Gibco) was incubated for 1 h at room temperature.

In order to identify biocytin (Sigma-Aldrich)-filled neurons, the fixed brain slices were incubated with streptavidin Cy3 (1:500; Jackson Immunoresearch, Hamburg, Germany) with 0.5% Triton X-100 (Roche) and 3% NGS (Gibco) for 1 h at room temperature.

Preparation of Acute Rat Brain Slices After Intrastriatal Transplantation of VM-Derived Progenitor Cells

Three to 12 weeks after intrastriatal transplantation of fetal rat VM progenitor cells, acute brain slices (300 μm thickness) were dissected. The transplanted rats were deeply anesthetized by exposure to isoflurane (Baxter, München, Germany). Under deep unconsciousness, rats were quickly decapitated and the head immersed in ice-cold sucrose solution [1 M NaCl (J.T. Baker), 2.5 M sucrose (Roth, Karlsruhe, Germany), 1 M $NaHCO_3$ (Merck), 1 M KCl (Merck), 0.5 M NaH_2PO_4 (Fluka), 0.05 M $CaCl_2$ (Sigma-Aldrich), 1 $MgCl_2$ (J.T. Baker), and 1 M glucose (Sigma-Aldrich)]. The following procedure was performed under cooled conditions. The brain was quickly removed; the cerebellum and brainstem were chopped off by a razor blade and pasted onto the vibratome holder (Hyrax V50; Carl Zeiss MicroImaging GmbH Jena, Germany) filled with ice-cold sucrose solution. The brain slices were cut (300 μm thick) and placed onto a nylon-covered holding (constructed by "Werkstätten" Hannover Medical School) surrounded by carbogen (O_2 95%/CO_2 5%; Linde, Hannover, Germany) fumigated sucrose solution at room temperature. Prior to recording, brain slices were incubated for 15 min at 37°C. Slices were transferred to the recording chamber and were constantly bathed with carbogen (Linde)-fumigated ACSF solution. To avoid sliding of the compound, the slices were held by a nylon stringed holder. The micropipette for patch clamp recording was immerged in the brain slice with applied positive pressure of approximately 10 mbar (Manometer PCE P15; PCE Instruments, Southampton, UK). The neurons within the eGFP-Flag-transfected graft were recorded under visual control (fluorescence microscope; Leica DM LFSA).

Electrophysiological Recording

Whole-cell patch clamp recordings were performed in vitro and in acute brain slices using ACSF bath solution. Pipettes with resistances of 5–8 MΩ were pulled from borosilicate glass capillaries (GC150-15; Harvard Apparatus, Hugstetten, Germany) using a pipette puller (Model P-97; Sutter Instruments, Novato, CA, USA) and fire polished (Microforge MF-830; Narishige, East Meadow, NY, USA). They were filled with intracellular solution containing 120 mM K-gluconate (Sigma-Aldrich), 10 mM NaCl (J.T. Baker), 0.25 mM $CaCl_2$ (Sigma-Aldrich), 5 mM EGTA (Roth), 2 mM $MgCl_2$ (J.T. Baker), 0.4 mM GTP (Sigma-Aldrich), 10 mM HEPES (SERVO), 10 mM glucose (Sigma-Aldrich), and 2 mM diNa-ATP (Sigma-Aldrich). One percent biocytin (Sigma-Aldrich) was added in order to visualize the penetrated neurons inside the graft. Current clamp measurements were performed using an Axopatch 200B amplifier (Axon Instruments, Union City, NJ, USA).

Analysis of Electrophysiological Data

The data were analyzed using Clampfit software (Version 10.2.0.14; Axon Instruments). Spontaneous activity was recorded continuously for 3 min (low-pass filter frequency 2,000–5,000 Hz; sampling rate 20 kHz). We intracellularly applied negative current steps to evoke hyperpolarizations below −100 mV, since DA-like neurons typically respond with a voltage "sag" to such stimuli. In order to characterize rectifying currents, the current–voltage relationship was determined at the most negative point in the early phase and after 485–495 ms in the late phase of the stimulation. The difference between membrane potentials of the early and the late phase (ΔmV) was plotted against the potential of the early phase. Neurons exhibiting a prominent deflection of the membrane potential over the period of stimulation indicate anomalous rectification (12). Additionally, cell responses were evoked by depolarizing and hyperpolarizing current steps between −1 nA and +1 nA (500 ms). Single action potential properties were investigated including the threshold (point of maximum rising in the depolarization phase), overshoot (maximal point of depolarization), spike heights (distance between overshoot and maximum of hyperpolarization), afterhyperpolarization amplitude (maximum of hyperpolarization), and spike duration (half heights of a single spike). Comparison of the membrane potential properties was performed using the Kruskal–Wallis and Dunn's multiple comparison test (GraphPad Prism).

RESULTS

Electrophysiological Recording of Intrastriatally Transplanted eGFP-Flag-Transfected Rat VM-Derived Progenitor Cells

In the first experiments, electrophysiological recordings were performed on brain slices of 6-OHDA-lesioned rats intrastriatally transplanted with rat VM progenitor cell suspensions, which had been transfected with eGFP-Flag to

allow visual identification of the graft (Fig. 1, exp. i). The eGFP-Flag neurons were evenly distributed throughout the graft (Fig. 2A, E, I) and could be detected for up to 12 weeks after grafting (data not shown). Transfected neurons were excluded from whole-cell patch clamp recordings, since eGFP-Flag (Fig. 2B, F, J) and TH-immunoreactive (ir) (Fig. 2C, G, K) neurons revealed no overlap (Fig. 2D, H, L), which is in accordance with our previous study (33). TH-ir neurons displayed a neuronal morphology already at early time points (3 to 5 weeks after grafting) (Fig. 2C), forming fusiform cell bodies with long neurite outgrowth. Recorded neurons were selected according to their location inside the graft. Again, in line with previous observations (33), TH-ir neurons were located in the core of the graft within the first 5 weeks (Fig. 2A) and at later posttransplantation intervals within the border of the graft (Fig. 2E, I). Especially at these late stages, eGFP-Flag-transfected neurons proved to be valuable to visualize the graft.

Responses of intrastriatally transplanted neurons (Fig. 1, exp. i, total number of recorded cells $c = 59$) were examined upon intracellular stimulation by hyperpolarizing currents. A hyperpolarization-activated inward current causes a bipolar deflection of the membrane potential at strong hyperpolarizations that is typical for pacemaker neurons. Since DA neurons naturally contain hyperpolarization-activated HCN channels, all mature DA neurons should display pacemaker characteristics with this potential rebound at highly negative potentials. Using this attribute, the recorded neurons were divided into putative DA and non-DA neurons. Figure 3A–C displays representative recordings of neurons derived from eGFP-Flag-transfected intrastriatal grafts. Type 1 (Fig. 3A) and type 2 (Fig. 3B) neurons displayed a voltage "sag" when negative currents were applied in the current clamp mode. Current steps evoked an early strong hyperpolarization that was attenuated after 100–200 ms leading to a repolarizing shift toward resting membrane potentials. Selectively performed voltage clamp recordings confirmed a distinct inward current at negative potentials below 90–100 mV (data not shown). Type 1 and 2 neurons typically showed a peak during the early phase of hyperpolarization. Figure 3D–F displays representative current–voltage relationships of the early and late phase response to hyperpolarizing stimuli. To compare the different groups of neurons, the difference (ΔmV) between the hyperpolarized membrane potential of the early and the late phase was plotted against the membrane potential of the early phase (Fig. 3G–I). Data were collected from recordings between 3 and 12 weeks after grafting. We did not observe any dependence on the intervals

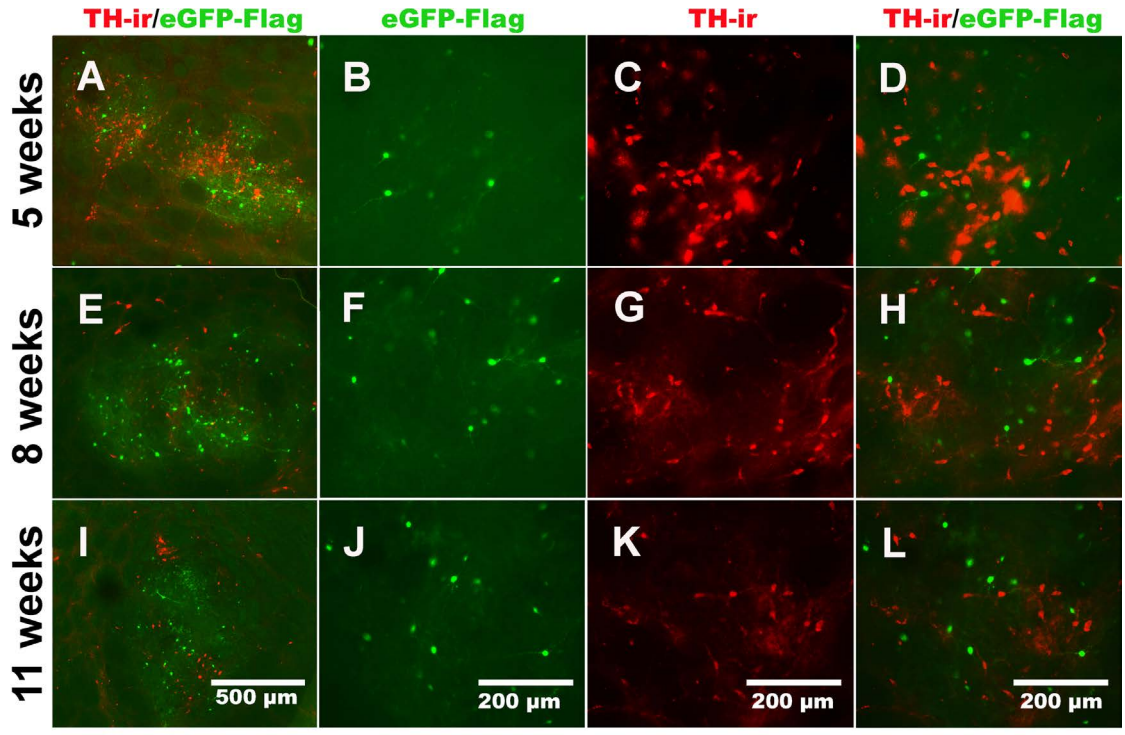

Figure 2. Validation of eGFP-Flag-transfected VM grafts 5 to 12 weeks after transplantation. eGFP-Flag-transfected neurons were distributed throughout the graft and detectable for up to 12 weeks after transplantation (A, E, I). Magnified eGFP-Flag (B, F, J) and TH-ir (C, G, K) neurons illustrate no overlap in the merged pictures (D, H, L). Five weeks after transplantation, TH-ir cells are distributed throughout the graft (A). Eight and 11 weeks after grafting, multiple TH-ir neurons are located at the border of the graft (E, I).

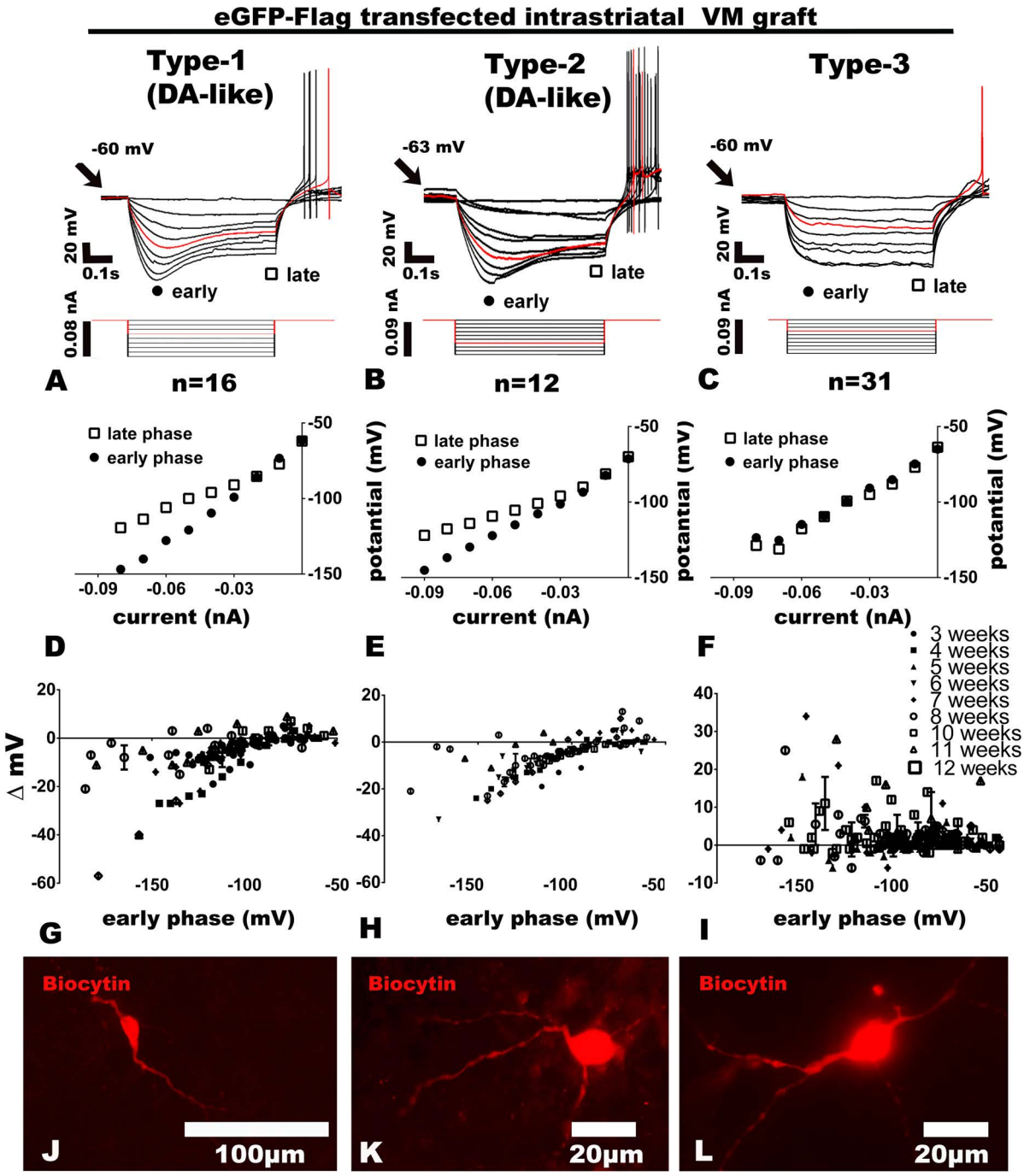

Figure 3. Grouping of the grafted neurons according to their response to hyperpolarizing current injection. Type 1 (A) and type 2 (B) neurons displayed a biphasic progression to hyperpolarization. Type 3 neurons showed simple, monophasic responses to hyperpolarizing stimuli (C). Type 1 neurons ($n=16$) showed no or delayed single spikes after hyperpolarization. Type 2 ($n=12$) exhibited fast repetitive spikes (bursts) after hyperpolarization (arbitrary spikes after hyperpolarization are highlighted in red, A, B). Representative current–voltage relationships of the early (dots) and the late phase were shown for each group (D, E, F). The voltage difference (Δ mV) between the early and the late phase (square) was plotted against the membrane potential of the early phase (G, H, I). ΔmV was examined in response to steps of hyperpolarizing stimuli and displayed for different intervals after grafting (3 to 12 weeks). Type 1 (G) and type 2 (H) neurons showed a deflection of the negative membrane potential beginning at −100 mV in the early phase. Type 3 neurons (I) showed no deflection of the negative membrane potential. There was no significant difference in ΔmV regarding time intervals after grafting. Two biocytin-labeled type 1 neurons could be characterized by a fusiform, bipolar morphology (J). Type 2 neurons were shown to have a round cell soma with two or more dendrites ($n=3$, K). (L) A single example for a highly branched neuron of the heterogeneous type 3 group that additionally implies bipolar, fusiforme ($n=2$), and round-shaped neurons ($n=3$).

after grafting. Both type 1 (Fig. 3G) and type 2 (Fig. 3H) neurons showed a deflection of the negative membrane potential beginning at −100 mV. In contrast, type 3 neurons showed no negative deflection at highly negative membrane potentials and no peak during the early phase of the hyperpolarization. An apparent positive deflection of ΔmV (Fig. 3I) results from the arbitrarily selected time for measurement of early phase potentials at 500–700 ms after stimulation, where hyperpolarization had not reached steady-state conditions in every cell (Fig. 3C).

We attempted to identify the recorded neurons by adding biocytin to the intracellular solution, which diffused inside the recorded neurons. However, in line with a previous study of Zhang et al., double labeling of biocytin and TH-ir neurons was not observed (47) after 15–20-min recording duration of single neurons. It is likely that the intracellular solution replaces the cytosol, since short 3-min recordings of putative DA neurons allow double labeling (24,47). Therefore, only sporadic labeling of recorded neurons was performed; nevertheless, these neurons demonstrate differences in their morphology, which might correspond to their electrophysiological properties. Two biocytin-labeled type 1 neurons exhibited a fusiform, bipolar morphology (Fig. 3J). Type 2 neurons were shown to have a round cell soma with two or more dendrites ($n=3$) (Fig. 3K). Type 3 neurons revealed different varieties of cell morphologies ($n=6$) (Fig. 3L). Figure 3L represents a single example for a highly branched neuron. Additionally, bipolar fusiform neurons ($n=2$) and round-shaped neurons ($n=3$) were detected, suggesting that several different cell types are associated within the type 3 classification.

Type 1 neurons ($n=16$) showed no ($n=10/16$) or delayed single spikes after hyperpolarization ($n=6/16$) (Fig. 3A). Type 2 neurons ($n=12$) attracted attention by discharging with fast repetitive spikes (bursts) after hyperpolarization (Fig. 3B). Type 3 ($n=31$) neurons showed no hyperpolarization-activated currents and no voltage "sag" in the current clamp mode, although strong hyperpolarization (below −150 mV) was induced (Fig. 3C).

Type 1 and type 2 neurons represent putative DA neurons and were examined for properties such as spontaneous activity (irregular and regular firing), pacemaker activity, and general characteristics of the membrane potential. Type 3 neurons are not considered as DA due to the lack of inward currents induced by hyperpolarization. This group is potentially consisting of a conglomeration of different types of neurons. Therefore, the membrane potentials and the spontaneous firing pattern display great variances. These neurons were excluded from further contemplations.

Type 1 Neurons—Spontaneous Activity

Overall, 33% of the evaluated intrastriatally transplanted neurons showed spontaneous action potentials, whereas 9% were represented by type 1 neurons, and 7% were represented by type 2 neurons. Type 1 neurons were either silent or exhibited an irregular, spontaneous firing mode (5 of 16 measured type 1 neurons; Fig. 4A). The occurrence of spontaneous activity was independent of the time point after grafting. Spontaneous activity occurred 3, 5, and 11 weeks after grafting. The firing pattern was characterized by interspike interval (ISI) histograms (35). Irregular firing resulted in broadly distributed spike intervals in the histogram (Fig. 4B). Type 1 neurons responded to depolarizations with high- or low-frequency spike trains depending on the intensity of stimulation (Fig. 4C). The frequency of irregular fired, spontaneous action potentials varied between 0.6 and 1.8 Hz (Table 1). Frequencies between 0.6 and 1.1 Hz ($n=3$) were measured 3 weeks after grafting, whereas 5 weeks after grafting, a frequency of 1.5 Hz ($n=1$) and 11 weeks after grafting 1.8 Hz ($n=1$) was recorded. This might indicate a slight increase in the firing frequency over time intervals after grafting. Nevertheless, due to the slow number of spontaneously active neurons, this needs to be proven in further investigations. The analysis of single spike properties of type 1 neurons displayed distinct afterhyperpolarization amplitudes (range between 52 mV and 37 mV) (Table 2) and spike durations between 1.1 and 2 ms. Intrinsic membrane properties are summarized in Table 2.

Type 2 Neurons—Spontaneous Activity

Type 2 neurons were either silent or discharged spontaneously in a regular ($n=2$) (Fig. 4D) or bursting manner ($n=2$). A regular firing pattern displayed a narrow, single-peaked distribution of intervals (Fig. 4E). All neurons displayed repetitive firing after steps of depolarizing currents (Fig. 4F). Burst firing is characterized by fast repetition of at least three discharges (Fig. 4G), which are illustrated in the ISI histogram by a peak at very short intervals (Fig. 4H). The appearance of spontaneous activity was independent of the duration after grafting. A burst firing was measured already 4 weeks after transplantation (mean of three event frequencies of single burst discharges 9 ± 4 Hz; event frequency 0.2 ± 0.2 Hz) and increased 8 weeks after grafting (mean event frequency of bursts 23 ± 8 Hz; event frequency 3 ± 13 Hz). Regular firing was measured 6 (4 ± 4 Hz) and 11 (3 ± 6 Hz) weeks after grafting and was characterized by a slow depolarization between spikes and a prominent afterhyperpolarization typical for pacemaker neurons.

The frequency of the regular firing pattern remained similar 4 and 11 weeks after transplantation, whereas the frequency of the spontaneously bursting neurons appeared to increase. Again, the small number of spontaneously active neurons did not allow correlations between time intervals after grafting and firing frequencies. The firing and membrane potential characteristics are summarized

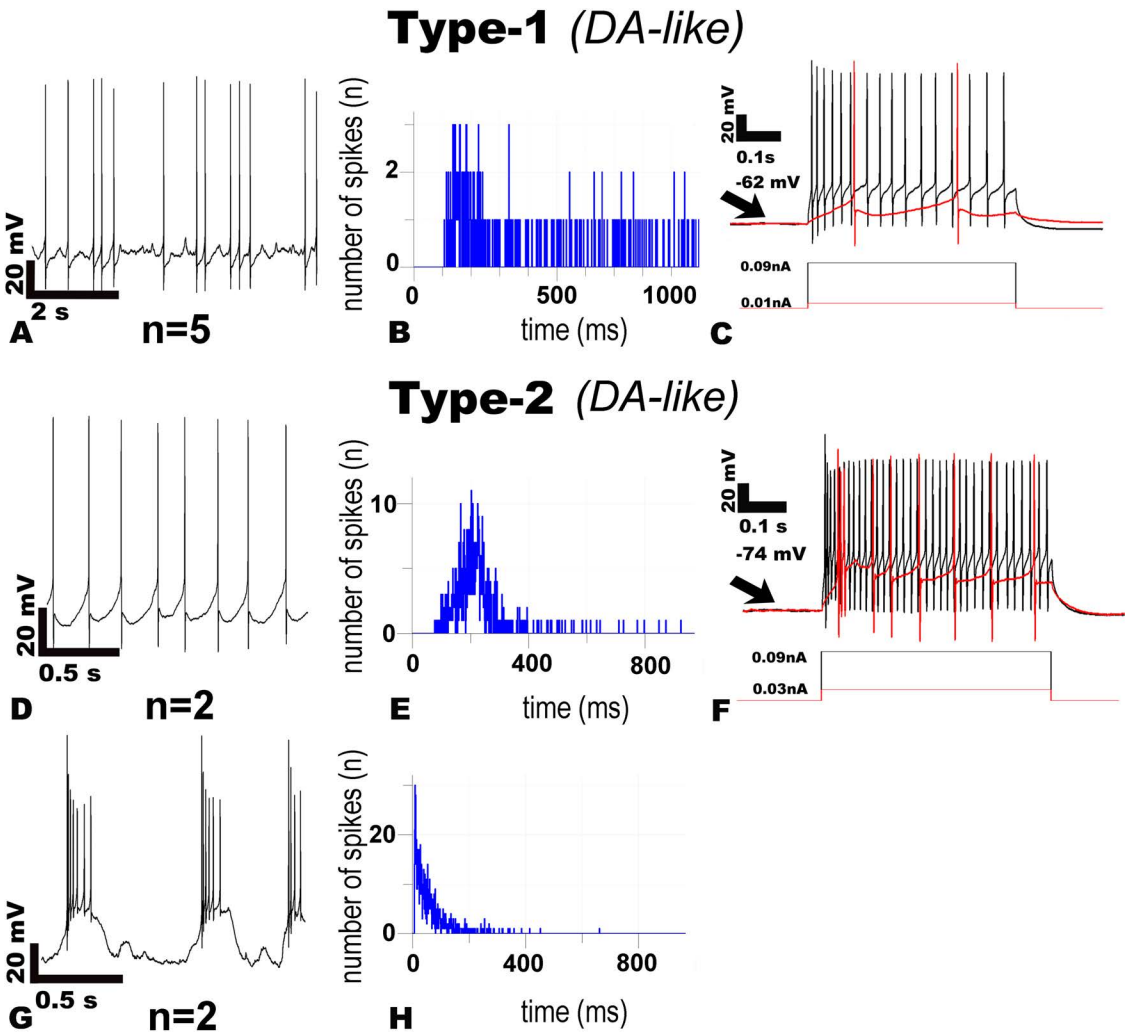

Figure 4. Representative spontaneous firing pattern of type 1 and type 2 neurons. Five out of 16 measured type 1 neurons exhibited irregular firing patterns (A), which were characterized by a broad distribution of intervals in the ISI histogram (B). Stimulation by depolarizing currents evoked repetitive firing (C). Type 2 neurons generated regular ($n = 2/12$) (D) and burst firing ($n = 2/12$) (G). Type 2 neurons displayed a repetitive firing mode at evoked responses (F). Regular firing pattern exhibited a narrow, single peak in the ISI histogram (E). With bursting neurons the single peak in the histogram is shifted to very short intervals (25 ms) (H).

in Table 2. Single spike properties were characterized by distinct afterhyperpolarization amplitudes (range between 56 and 28 mV) (Table 2) and spike durations from 1 to 1.8 ms (Table 2).

Properties Type 1 Neurons—Postsynaptic Potential

The input resistance of type 1 neurons was determined from voltage shifts evoked by current injections of small amplitude and ranged from 250 MΩ to 2.5 GΩ. This variance was independent of the duration after grafting and could not be used to estimate neuronal maturation or integration. However, some neurons of both classes, type 1 and type 2, displayed spontaneous postsynaptic potentials (PSPs) that indicate formation of new interconnections of the singularized transfected cells within the graft or with neurons of the surrounding host tissue. Figure 5A is a representative measurement of spontaneous PSPs from a type 1 neuron. In the upper panel, the spontaneous activity was recorded for 165 s. Episodes with single and multiple PSPs result in depolarization and generation of single action potentials or trains of discharges. The PSPs are magnified in the lower panel showing multiple PSPs with peaks up to 4 mV. PSPs occurred in measurements at early (3 weeks) and late (11 weeks) time points after grafting.

Properties Type 2 Neurons—Postsynaptic Potential

The input resistance ranged between 400 MΩ and 1.5 GΩ. No correlation between time after grafting and input resistance could be found. Synaptic integration is illustrated in Figure 5B by the occurrence of PSPs. In the

Table 1. Spontaneous Firing Frequency (Hz) of the Intrastriatally Grafted VM Progenitor Cells Obtained 3–11 Weeks After Transplantation

Weeks After Transplantation	3	4	5	6	8	11
Type 1 neurons (Hz)	0.6 ± 1.4 (irregular) 0.6 ± 1.5 (irregular) 1.1 ± 1.6 (irregular)		1.5 ± 14 (irregular/burst)			1.8 ± 3 (irregular)
Type 2 neurons (Hz)		0.2 ± 0.2 (bursting) mean single bursts 9 ± 4		4 ± 4 (regular)	3 ± 13 (bursting) mean of single bursts 23 ± 8	3 ± 6 (regular)
TH-GFP in situ (Hz)			2 ± 1 (irregular)			

VM, ventral mesencephalon; TH-GFP, tryosine hydroxylase-green fluorescent protein.

Table 2. Characteristics of Single Evoked Action Potentials

	Type 1 ($n=16$)	Type 2 ($n=12$)	TH-GFP In Vitro ($n=12$)	TH-GFP In Situ ($n=6$)
Resting membrane potential (mV)	−64 Q 1.: −69 Q 2.: −58 ($n=9$)	−66 Q 1.: −69 Q 2.: −58 ($n=9$)	−59 Q 1.: −67 Q 2.: −54	−61 Q 1.: −70 Q 2.: −53
Threshold (mV)	−36 Q 1.: −40 Q 2.: −29 60 **	−35 Q 1.: −40 Q 2.: −33 60 *	−34 Q 1.: −37 Q 2.: −31 36	−28 Q 1.: −33 Q 2.: −22 41
Overshoot (mV)	Q 1.: 49 Q 2.: 68	Q 1.: 50 Q 2.: 65	Q 1.: 27 Q 2.: 47	Q 1.: 33 Q 2.: 59
AHP-amplitude (mV)	−34 Q 1.: −43 Q 2.: −28 129 **	−31 Q 1.: −43 Q 2.: −26 132 **	20 Q 1.: −37 Q 2.: −13 91	26 Q 1.: −47 Q 2.: −18 102
AP-heights (mV)	Q 1.: 112 Q 2.: 145	Q 1.: 118 Q 2.: 142	Q 1.: 75 Q 2.: 99 ($n=11$)	Q 1.: 84 Q 2.: 118
AP-duration (ms)	1.4 Q 1.: 1.1 Q 2.: 2	1.4 * Q 1.: 1 Q 2.: 1.8	2.5 Q 1.: 1.8 Q 2.: 2.9 ($n=11$)	2.1 Q 1.: 1.7 Q 2.: 2.6
Voltage "sag" to hyperpolarizing currents injection	16/16	12/12	7/9	5/5
Single spikes after hyperpolarization	6/16	0/12	0/9	0/6
Bursting discharge after hyperpolarization	0/16	12/12	0/9	0/6
Spontaneous activity	5/16	4/12	1/12	1/6
Regular firing pattern	0/16	2/12	1/12	0/6
Irregular firing	5/16	0/12	0/12	1/6
Burst firing	0/16	2/12	0/12	0/6
Input resistance (MΩ)	957 Q1: 267 Q2: 2300	710 Q1: 441 Q2: 945	1442 Q1: 778 Q2: 1680	750 Q1: 402 Q2: 1569

AHP, after hyperpolarization; AP, action potential.

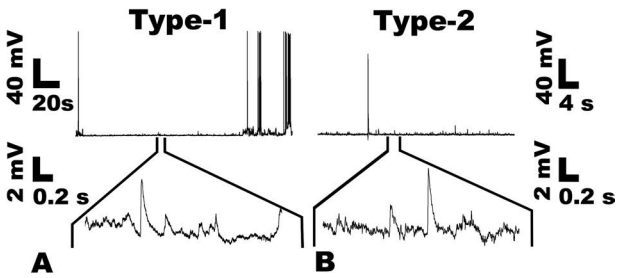

Figure 5. Synaptic input of type 1 and type 2 neurons. The upper panel illustrates receiving PSPs inducing bursting discharge in type 1 neurons (A). In the lower panel, the magnified excerpt demonstrates single and multiple PSPs. Type 2 neurons receive PSPs as well, which again induce discharging, in this case sporadic APs (B). The lower panel again represents the magnified excerpt of the upper recording.

upper panel, a single AP is elicited. Large episodes possess trains of PSPs, which seems to sporadically induce APs. These trains are visualized in the magnification in the lower panel of Figure 5B. PSPs occurred in measurements at early (3 weeks) and late (11 weeks) time points after grafting.

The firing frequencies and other electrophysiological parameters are summarized in Tables 1 and 2.

Electrophysiological Recording of Genetically Identified DA Neurons In Vitro Derived From TH-GFP Transgenic Mice

Since double labeling of biocytin-filled neurons with a TH-antibody failed, a direct correlation of TH-ir cells with electrophysiological properties was not possible. To directly characterize DA neurons, neurons expressing GFP under the control of the TH-promotor were recorded in dissociated cell cultures derived from tgTH-GFP mice and after intrastriatal transplantation into the 6-OHDA rat PD model (Fig. 1, exp. ii).

Anti-TH ICC revealed a complete overlap of GFP fluorescent cells with TH-ir neurons in vitro. Figure 6A shows an example for TH-ir neurons expressing GFP, which were characterized by a fusiform bipolar morphology; however, not all TH-ir cells were GFP positive, which is in accordance to a previous study (25). GFP-expressing neurons were electrophysiologically characterized using the same protocols as for rat progenitor cells.

In a first approach, TH-GFP neurons were cultured and investigated in vitro. Nine TH-GFP neurons were stimulated by hyperpolarizing current steps in the whole-cell current clamp mode. Such TH-GFP neurons in vitro demonstrated a clear voltage "sag" to hyperpolarizing current

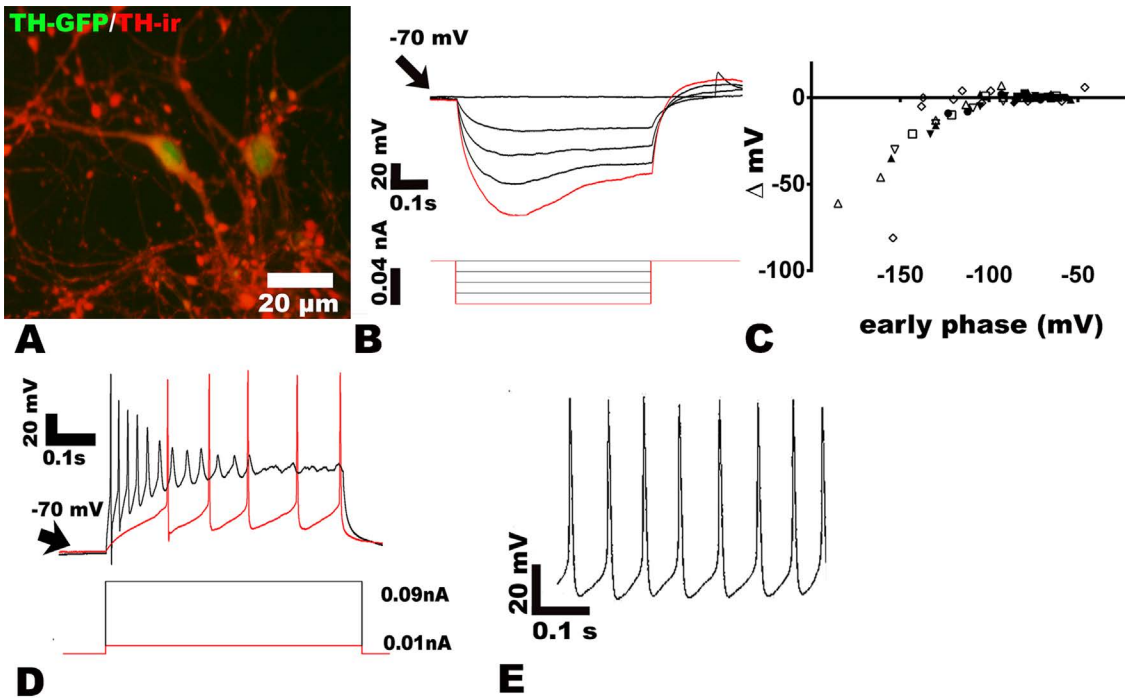

Figure 6. Whole-cell patch clamp recordings of genetically labeled DA neurons derived from transgenic TH-GFP mice in vitro. Six days after differentiation, TH-GFP neurons revealed a complete overlap of GFP and TH-ir neurons (A). Seven out of nine TH-GFP neurons in vitro demonstrated a clear biphasic response to a stimulation with hyperpolarizing currents ($n=9$, B, C). All TH-GFP-positive neurons generated spikes after depolarization (D). A regular discharge pattern of the single TH-GFP neuron in vitro that was spontaneously firing (E).

injections as illustrated in Figure 6B. Most neurons (7/9) reaching membrane potentials of at least −120 mV displayed a prominent deflection of the membrane potential over the period of stimulation (Fig. 6C).

All GFP-positive neurons (12 out of 12 measured) generated spikes after stimulation with depolarizing currents (Fig. 6D). The neurons could be excited at thresholds around −47 mV with long action potential durations ranging from 1.8 to 2.9 ms and prominent afterhyperpolarization amplitudes (range from 50 to 26 mV) (Table 2). Spontaneous activity could only be observed for a single TH-GFP neuron in vitro (12 ± 8 Hz) (Fig. 6E). This regular firing neuron displayed repetitively depolarizing membrane potentials and spikes with prominent afterhyperpolarizations (Fig. 6E).

Electrophysiological Recording of Intrastriatally Transplanted Genetically Identified DA Neurons Derived From Cell Suspensions of TH-GFP Transgenic Mice

Experiment iii (Fig. 1) was performed to allow comparison of in situ measurements of identified DA neurons with the data from experiment i (Fig. 1), recorded from grafted rat progenitor cells. Therefore, VM-derived cell suspensions of tgTH-GFP mice were intrastriatally transplanted into adult 6-OHDA-lesioned rats and recorded 6 weeks after transplantation (Fig. 7). IHC confirmed the complete overlap of GFP-expressing TH-GFP neurons in situ and TH-ir neurons (Fig. 7A–C), and their typical location near the border of the graft. The higher magnification illustrates the bipolar and fusiform morphology of TH-GFP neurons in situ (Fig. 7D).

Recordings of grafted tgTH-GFP neurons resulted in a voltage "sag" to hyperpolarizing current injections for all measured neurons ($n = 6$) (Fig. 7E). ΔmV demonstrates these voltage "sags" (Fig. 7F). Only one neuron generated spontaneous discharges in an irregular manner (2 ± 1 Hz) (Table 1) (Fig. 7G). Neither delayed spikes nor bursts after hyperpolarization occurred. All measured neurons generated spikes in response to depolarizing current steps (Fig. 7H). The neurons generated spikes at approximately −28 mV with long durations ranging between 1.7 and 2.6 ms and prominent afterhyperpolarization amplitudes (range: 56 and 28 mV) (Table 2). In order to verify the functional integration of the xenografts, staircase tests were performed. The ability of the rats to grasp sugar pellets from each stair with the contralateral and ipsilateral paw was investigated with the paw-reaching test. Six out of 16 lesioned rats displayed a preference to the ipsilateral paw compared to the contralateral paw. These six rats were chosen to receive a TH-GFP xenograft. Five weeks after grafting, two kinds of analyses were performed. First, the paw-reaching test of the affected contralateral paw (Fig. A,B) was measured. Two out of six rats revealed significantly improved motor skills after grafting ($p < 0.05$ or 0.01, respectively) (Fig. 8A). Second, the farthest distance reached was analyzed in the reached distance test. Three rats exhibited improved motor skills of the contralateral

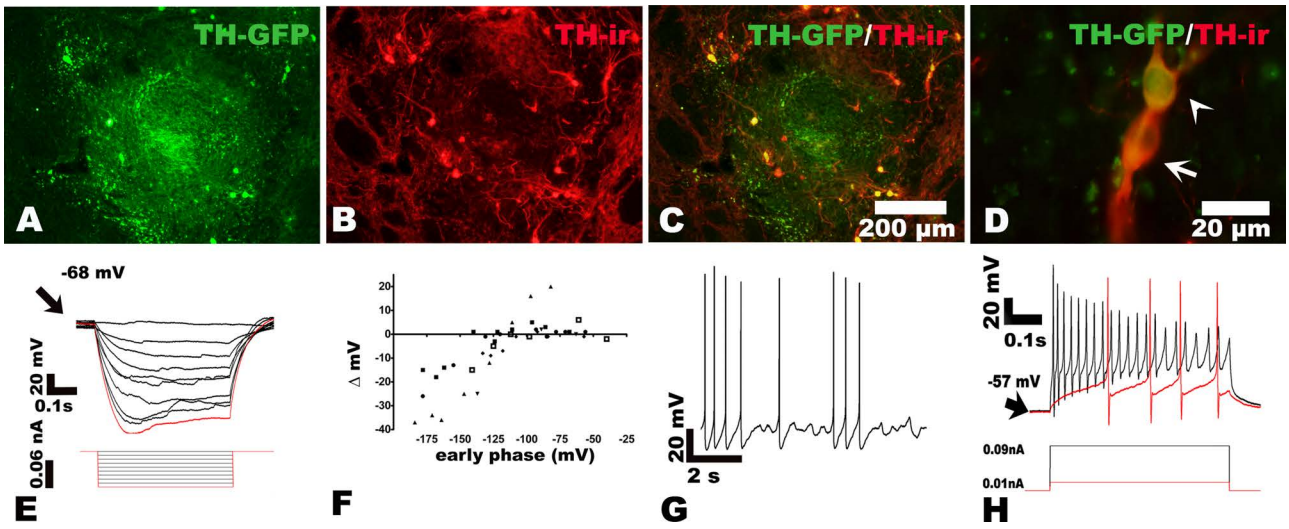

Figure 7. TH-GFP neurons 6 weeks after transplantation. GFP-expressing (A) and TH-ir neurons (B) are located at the border of the graft. All GFP neurons are colabeled with TH-ir neurons, whereas not all TH-ir neurons express GFP (C). Higher magnification illustrates the bipolar and fusiform morphology of the GFP-expressing neurons (arrowhead) and TH-ir neurons (arrows) after grafting (D). Recordings of grafted TH-GFP neurons expressing GFP showed a biphasic response to stimulation with hyperpolarizing currents (E). The difference of the early to the late phase of the hyperpolarization (ΔmV) demonstrates a distinct deflection of the early toward the late phase (F). One grafted neuron generated spontaneous discharges in an irregular manner (G). All measured neurons generated spikes after depolarization (H).

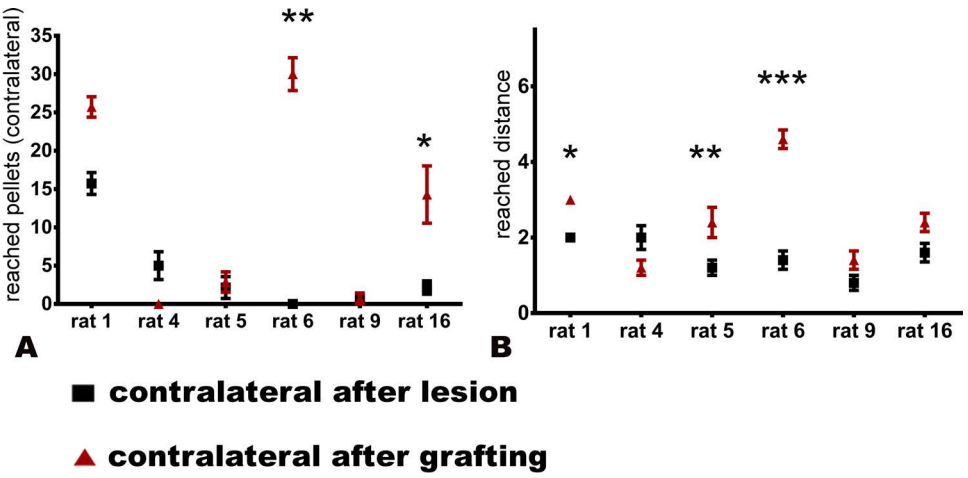

Figure 8. Analysis of the affected contralateral paw after lesion and after grafting. The staircase test session 4 weeks after transplantation of the rats revealed significantly improved motor skills of the contralateral paw according to the reached pellets test (2 out of 6, A) and reached-distance test (3 out of 6, B) compared to the staircase test session after lesion (*$p<0.05$, **$p<0.01$, ***$p<0.001$).

paw ($p<0.05$, 0.01, or 0.001, respectively) (Fig. 8B) compared to the ipsilateral paw. One of the rats (#6) showed significant improvement in the paw-reaching test and in the reached distance test. Electrophysiological recordings were performed with two rats showing improvements in the reached distance test (#5, #6) and with one rat showing no significant behavioral improvement at all (#4). No significant difference in electrophysiological properties could be observed between the improved rats #5, #6 and the not improved rat #4. Nevertheless, spontaneous activity was recorded in one rat (#5), which showed improvements in the reached distance test.

Comparison of the Electrophysiologically Characterized DA-Like Cells

Comparison of the electrophysiologically characterized putative DA-like cells in the rat VM-progenitor cell grafts (experiment i, Fig. 1) with identified tgTH-GFP neurons (experiments ii and iii, Fig. 1) showed that type 1 neurons and type 2 neurons exhibited hyperpolarization-activated rectification. This is the most conspicuous property of DA neurons since all TH-GFP neurons in vitro and in situ exhibited voltage "sags" upon hyperpolarizing current injections (Figs. 6, 7). Differences between type 1 and type 2 neurons arose for the discharge behavior after hyperpolarization. Type 1 neurons revealed delayed spikes (Fig. 3A) and type 2 neurons burst after hyperpolarization (Fig. 3B). However, no bursts or delayed spikes could be observed for TH-GFP neurons in vitro (Fig. 6B) or after intrastriatal transplantation (Fig. 7E).

Both type 1 and type 2 neurons exhibited spontaneous spike discharges, whereas tgTH-GFP neurons in vitro displayed regular firing (Fig. 6E) similar to type 1 neurons. Type 2 neurons resemble in their spontaneous activity the tgTH-GFP neurons after grafting, which fired irregularly (Fig. 7G). No bursting behavior could be recorded for type 1, TH-GFP in vitro, and in situ neurons.

In conclusion, type 1 and type 2 neurons exhibited similar properties as identified DA neurons of tgTH-GFP mice. Depending on the age of the graft, type 1 and type 2 neurons exhibited a slight increase in the spontaneous firing frequency, which might reflect a progressive integration of the grafted DA neurons. Type 1 and type 2 neurons received input by surrounding neurons or the host striatum represented by PSPs 3 to 11 weeks after grafting. The input resistances were similar in all groups of the grafted putative DA neurons and the identified DA neurons. No correlation could be made between input resistance and time point after grafting. Nevertheless, it is reasonable to conclude that varying resistances indicate different levels of maturation and integration on the single cell level.

DISCUSSION

Here we show electrophysiological properties of grafted VM progenitor cells over a period of 3 to 12 weeks after transplantation measured in acute brain slices using eGFP-Flag transfection to identify the graft. We were able to classify typical electrophysiological features of DA neurons based on their firing properties in correlation to features of the short-term differentiated genetically labeled DA neurons in vitro and 6 weeks after grafting. The improved motor functions of the contralateral forelimb of TH-GFP-grafted rats were demonstrated by the staircase tests 6 weeks after grafting. As previous studies showed, restoration of the motor function can occur

2 to 12 weeks after grafting depending on the graft size (22). We showed that amphetamine- and apomorphine-induced rotations revealed a progressive behavioral improvement 3 to 12 weeks after transplantation (33). Electrophysiological recordings revealed functional DA properties of eGFP-Flag-transfected progenitor cells in the host brain. Nevertheless, identification of the recorded neurons of the eGFP-Flag-transfected rat VM progenitor cells by double labeling with biocytin-filled neurons and TH-ir neurons failed. It is likely that the intracellular solution replaces the cytosol like it was shown in a study of Zhang et al. (47). Therefore, DA-like characteristics of type 1 and type 2 neurons were confirmed by recordings of the identified DA neurons (tgTH-GFP) in vitro and in vivo after intrastriatal xenotransplantation.

We used the occurrence of voltage sag to identify DA neurons. This typical property of DA neurons was also described for mature DA neurons of the SNpc (18). They are induced by hyperpolarization-activated cyclic nucleotide gated cation channels (HCN), which enable small depolarizing currents generating repetitive firing in pacemaker neurons (44). Dopaminergic neurons of the medial ventral tegmental area, however, were described to display a reduced sag potential compared to DA neurons of the SN (47).

Previous studies concerning the electrophysiological characterization of transplanted VM neurons included blind recordings via additional holes in anesthetized rats (8,20). Fisher et al., for example, described a group of DA neurons firing spontaneously in a regular and irregular manner (9); however, inward rectification as a major characteristic of DA neurons (14,34,35) could not be recorded. The study of van Horne et al. was also performed blindly in anesthetized rats (43). Grafted neurons were identified by comparing firing properties to rat DA neurons, but again, inward rectification was not recorded (43). Sorensen et al. recorded voltage "sag" as a response to hyperpolarizing currents in identified tgDA neurons 21–36 days after grafting into the lesioned neonatal rat striatum in acute brain slices (39). Previous recordings of SNpc organotypic cultures revealed no hyperpolarization-activated inward current (6) in contrast to acute brain slices. The hyperpolarization-activated inward current of postnatally recorded neurons increased until the postnatal day 5 (45). According to this electrophysiological property, we classified three types of neurons. Sag potentials could be recorded in type 1 and type 2 neurons 3 to 12 weeks after grafting. The degree of the deflection was independent on the time point after grafting.

Type 2 neurons differed by the bursting discharge after hyperpolarization. Bursting is often described as a property of DA neurons (18). DA neurons within the SN in vivo are reported to fire in three different patterns: regular, irregular, and burst firing (16,17), which play a key role in the regulation of movement. Freely moving rats were shown to fire more frequently in a bursting manner than anesthetized or paralyzed rat preparations (11). Burst firing modulates a phasic release of dopamine-regulating fast movements (18). It has never been observed, neither in in vitro recordings (20) nor in acute brain slices (39). In in vitro studies, only silent or regular firing DA neurons were recorded (20). In agreement to these previous observations, in our study, DA neurons in vitro were silent except for a single DA neuron displaying a regular firing pattern. Others have shown that DA neurons derived from tgTH-GFP neurons grafted into the postnatal lesioned rat striatum reported to exhibit 75% spontaneous activity nearly similar to DA neurons of the SN in vivo, but displayed nearly completely a regular firing pattern (39). According to many electrophysiological studies, DA neurons within the SNpc in organotypic or dissociated cell cultures display main characteristics including the pacemaker activity marked by repetitive slow depolarization, prominent afterhyperpolarization, and wide action potential durations ranging from 2 to 4 ms (13,34,35). However, the xenografted DA neurons derived from transgenic mice 6 weeks posttransplantation into the rat striatum were silent with the exception of a single DA neuron exhibiting an irregular firing pattern. In contrast, rat VM-derived neurons transplanted into the rat striatum displayed irregular (type 1), regular, and burst firing patterns (type 2) similar to DA neurons of the SNpc in vivo. In our experiment, 5 out of 16 type 1 neurons fired irregularly. Regular or burst firing could not be recorded. Nevertheless, type 2 neurons fired mainly in a bursting pattern and to a minor degree regular. Especially in contrast to the identified DA neurons in vitro and 6 weeks after xenografting, the spontaneous activity of type 1 and type 2 neurons reflects features of mature DA neurons of the SNpc.

Additionally, irregular firing behavior and burst firing seem to be an indicator for endogenous inputs (12). Burst firing was recorded in organotypic cultures of the subthalamic nucleus, VM, and mesopontine tegmental explants (35) suggesting that the input of these brain areas plays a crucial role in the regulation of the firing pattern. Especially the subthalamic nucleus mediates burst firing by excitatory inputs to DA neurons of the SNpr (18,27). PSPs arose at recordings from 3 to 11 weeks after grafting in type 1 and type 2 neurons. PSPs induced partly single APs or even bursts indicating synaptic transmission from the host striatum and the surrounding neurons. These potentials prove a novel interconnection of the dissociated VM suspension inside the host brain. Functional synaptic integration of grafted DA neurons is fundamental for cell replacement therapy in PD. The regular and burst firing provides evidence of integrated DA neurons, which are substituting the missing endogenous DA input. Especially bursting and irregular firing seems to be a

reaction of DA neurons to the surrounding neuronal input (19). In vivo DA neurons of the SNpc receive inhibitory input by the GABAergic neurons of the striatum and the globus pallidus. Excitatory inputs derive from the medial prefrontal cortex, the STN, and the pedunculopontine tegmentum (18). Burst firing indicates a phasic stimulation of the striatal dopamine receptors (18), which might also be a response to a glutamatergic input. The *N*-methyl-D-aspartate receptor is reported to be relevant for the burst generation. Gain of the spike frequency throughout development is reported marking an ongoing maturation (40). In our study, the time course after grafting was independent of the occurrence of spontaneous activity. However, a slight increase in the irregular firing frequency of type 1 and bursting frequency of type 2 neurons was detected throughout the temporal intervals after grafting. This suggests a progressive advancement of the grafted DA neurons inside the host brain. There was also no correlation between firing pattern and grafting duration. Nevertheless, the low number of recorded spontaneous activity does not allow a conclusion whether the time course affects the excitability of the grafted neurons. DA neurons in vivo have an input resistance about 30–65 MΩ (16,21). In vitro recorded DA neurons have an increased input resistance ranging from 100 to 600 MΩ (5,21,35). This is in line with our recordings of DA neurons in brain slices and in in vitro cultures. The input resistances vary between 267 MΩ and 2.5 GΩ. Even though we did not find a correlation between input resistances and time after grafting, it appears reasonable that varying resistances indicate different levels of maturation and integration on the single cell level.

Type 1 neurons exhibited DA-like properties relating to the spontaneous and evoked potentials, which were also applied in previous experiments evaluating DA neurons within the SN (35). Regarding the single spike properties, there was no difference between type 1 and type 2 neurons. Nevertheless, in vitro recorded TH-GFP neurons exhibited distinctly wider spike durations than intrastriatally grafted type 1 neurons. Compared to TH-GFP neurons in vitro, a significant increase in the overshoot and the spike heights of type 1 and type 2 neurons could be observed. However, there were differences in the morphology of the biocytin-labeled type 1 neurons, which were in contrast to type 2 neurons bipolar and fusiform, similar to the GFP-expressing DA neurons in vitro and in situ. Examinations of DA-like neurons of labeled neurons were also described to be fusiform, ovoid, and of medium size (9).

In conclusion, electrophysiological examination of intrastriatally grafted neurons derived from VM progenitor cells revealed two types of neurons showing DA neuron-like properties. However, type 1 neurons were shown to possess in addition distinct electrophysiological and morphological characteristics of DA neurons in vitro and in vivo. They fired spontaneously in an irregular manner, indicating a high integration into the host brain even up to 12 weeks after grafting. Type 2 neurons differed by prominent spontaneous burst firing. Synaptic transmission potentially from the host striatum and the surrounding neurons is marked by PSPs. No difference in the maturation of the DA neurons could be detected over time intervals after grafting. It is likely that type 1 and type 2 neurons are actually DA neurons, which display an ongoing integration into the host striatum.

ACKNOWLEDGMENTS: We would like to thank Dr. Lorenz Müller and Professor Rüdiger Köhling for introducing us to the whole-cell patch clamp technique in acute brain slices (Institute of Physiology, University of Rostock). We also thank Professor Dr. P. Claus for the allocation of the high molecular weight FGF-2 protein, which was prepared under his guidance in the Institute of Neuroanatomy, Hannover Medical School. The authors declare no conflicts of interest.

REFERENCES

1. Barker, R. A.; Barrett, J.; Mason, S. L.; Björklund, A. Fetal dopaminergic transplantation trials and the future of neural grafting in Parkinson's disease. Lancet Neurol. 12:84–91; 2013.
2. Björklund, A.; Stenevi, U.; Schmidt, R .H.; Dunnett, S .B.; Gage, F .H. Intracerebral grafting of neuronal cell suspensions I. introduction and general methods of preparation. Acta Physiol. Scand. Suppl. 522:1–8; 1983.
3. Brewer, G.; Price, P. Viable cultured neurons in ambient carbon dioxide and hibernation storage for a month. Neuroreport 7:1509–1512; 1996.
4. Cesnulevicius, K.; Timmer, M.; Wesemann, M.; Thomas, T.; Barkhausen, T.; Grothe, C. Nucleofection is the most efficient nonviral transfection method for neuronal stem cells derived from ventral mesencephali with no changes in cell composition or dopaminergic fate. Stem Cells 24:2776–2791; 2006.
5. Chiodo, L; Kapatos, G. Membrane properties of identified mesencephalic dopamine neurons in primary dissociated cell culture. Synapse 11:294–309; 1992.
6. Cucchiaroni, M. L.; Freestone, P. S.; Berretta, N.; Viscomi, M. T.; Bisicchia, E.; Okano, H.; Molinari, M.; Bernardi, G.; Lipski, J.; Mercuri, N. B.; Guatteo, E. Properties of dopaminergic neurons in organotypic mesencephalic-striatal co-cultures-evidence for a facilitatory effect of dopamine on the glutamatergic input mediated by α-1 adrenergic receptors. Eur. J. Neurosci. 33:1622–1636; 2011.
7. Di Loreto, S.; Florio, T.; Capozzo, A.; Napolitano, A.; Adorno, D.; Scarnati, E. Transplantation of mesencephalic cell suspension in dopamine-denervated striatum of the rat. Exp. Neurol. 138:318–326; 1996.
8. Effenberg, A.; Klein, A.; Gibb, R.; Carroll, C.; Baumgärtner, W.; Grothe, C.; Ratzka, A. Adult hemiparkinsonian rats do not benefit from tactile stimulation. Behav. Brain Res. 261:97–105; 2013.
9. Fisher, L. J.; Young, S. J.; Tepper, J. M.; Groves, P. M.; Gage, F. H. Electrophysiological characteristics of cells within mesencephalon suspension grafts. Neuroscience 40:109–122; 1991.
10. Freed, C. R.; Greene, P. E.; Breeze, R. E.; Tsai, W.-Y.; DuMouchel, W.; Kao, R.; Dillon, S.; Winfield, H.; Culver,

S.; Trijanowsk, J. Q.; Eidelberg, D.; Fahn, S. Transplantation of embryonic dopamine neurons for severe Parkinson's disease. N. Engl. J. Med. 344:710–719; 2001.
11. Freeman, S. A.; Meltzer, T. L.; Bunney, B. S. Firing properties of substantia nigra dopaminergic neurons in freely moving rats. Life Sci. 36:1983–1994; 1994.
12. Grace, A. A. In vivo and in vitro intracellular recordings from rat midbrain dopamine neurons. Ann. NY Acad. Sci. 537:51–76; 1988.
13. Grace, A. A. Regulation of spontaneous activity and oscillatory spike firing in rat midbrain dopamine neurons recorded in vitro. Synapse 7:221–234; 1991.
14. 14.Grace, A. A.; Bunney, B. S. Intracellular and extracellular electrophysiology of nigral dopaminergic neurons-2. Action potential generating mechanisms and morphological correlates. Neuroscience 10:317–331; 1983.
15. Grace, A. A.; Bunney, B. S. Intracellular and extracellular electrophysiology if nigral dopaminergic neurons-3. Evidence for electrotonic coupling. Neuroscience 10:333–348; 1983.
16. Grace, A. A.; Bunney, B. S. Intracellular and extracellular electrophsiology of nigral dopaminergic neurons-1. Identification and characterization. Neuroscience 10:301–315; 1983.
17. Grace, A. A.; Bunney, B. S. The control of firing pattern in nigral dopamine neurons: Burst firing. J. Neurosci. 4:2877–2890; 1984.
18. Guatteo, E.; Cucchiaroni, M. L.; Mercuri, N. B. Substantia nigra control of basal ganglia nuclei. J. Neural Transm. Suppl. 73:91–101; 2009.
19. Hahn, J.; Kullmann, P. H. M.; Horn, J. P.; Levitan, E. S. D2 autoreceptors chronically enhance dopamine neuron pacemaker activity. J. Neurosci. 26:5240–5247; 2006.
20. Jomphe, C.; Bourque, M.-J.; Fortin, G. D.; St-Gelais, F.; Okano, H.; Kobayashi, K.; Trudeau, L.-E. Use of TH-EGFP transgenic mice as a source of identified dopaminergic neurons for physiological studies in postnatal cell culture. J. Neurosci. Methods 146:1–12; 2005.
21. Kita, T.; Kita, H.; Kitai, S. T. Electrical membrane properties of rat substantia nigra compacta neurons in an in vitro slice preparation. Brain Res. 372:21–30; 1986.
22. Lane, E. L.; Winkler, C.; Brundin, P.; Cenci, M. A. The impact of graft size on the development of dyskinesia following intrastriatal grafting of embryonic dopamine neurons in the rat. Neurobiol. Dis. 22:334–345; 2006.
23. Lindvall, O.; Brundin, P.; Widner, H.; Rehncrona, S.; Gustavii, B.; Frackowiak, R.; Leenders, K. L.; Sawle, G.; Rothwell, J. C.; Marsden, C. D.; Björklund, A. Grafts of fetal dopamine neurons survive and improve motor function in Parkinson's disease. Science 247:574–577; 1989.
24. Margolis, E. B.; Coker, A. R.; Driscoll, J. R.; Lemaître, A. I.; Fields, H. L. Reliability in the identification of midbrain dopamine neurons. PLoS One 5:e15222; 2010.
25. Matsushita, N.; Okada, H.; Yasoshima, Y.; Takahashi, K.; Kiuchi, K.; Kobayashi, K. Dynamics of tyrosine hydroxylase promoter activity during midbrain dopaminergic neuron development. J. Neurochem. 82:295–304; 2002.
26. Montoya, C. P.; Campbell-Hope, L. J.; Pemberton, K. D.; Dunnett, S. B. The "staircase test": A measure of independent forelimb reaching and grasping abilities in rats. J. Neurosci. Methods 36:219–228; 1991.
27. Nakanishi, H; Kita, H.; Kitai, S. T. Intracellular study of rat substantia nigra pars reticulata neurons in in vitro slice preparation: Electrical membrane properties and response characteristics to subthalamic stimulation. Brain Res. 437:45–55; 1987.
28. Nikkhah, G.; Eberhard, J.; Olsson, M.; Björklund, A. Preservation of fetal ventral mesencephalic cells by cool storage: In vitro viability and TH-positive neuron survival after microtransplantation to the striatum. Brain Res. 687:22–34; 1995.
29. Nikkhah, G.; Rosenthal, C.; Hedrich, H. J.; Samii, M. Differences in acquisition and full performance in skilled forelimb use as measured by the "staircase test" in five rat strains. Behav. Brain Res. 92:85–95; 1998.
30. Olanow, C. W.; Goetz, G. G.; Kordower, J. H.; Stoessl, A. J.; Sossi, V.; Brin, M. F.; Shannon, K. M.; Nauert, G. M.; Perl, D. P.; Godbold, J.; Freeman, T. B. A. Double-blind controlled trial of bilateral fetal nigral transplantation in Parkinson's disease. Ann. Neurol. 54:403–414; 2003.
31. Pape, H. C. Queer current and pacemaker: The hyperpolarization-activated cation current in neurons. Annu. Rev. Physiol. 58:299–327; 1996.
32. Paxinos, G.; Watson, C. The rat brain in stereotaxic coordinates. San Diego, CA: Compact. Acad. Press; 1997.
33. Ratzka, A.; Kalve, I.; Ozer, M.; Nobre, A.; Wesemann, M.; Jungnickel, J.; Köster-Patzlaff, C.; Baron, O.; Grothe, C. The colayer method as an efficient way to genetically modify mesencephalic progenitor cells transplanted into 6-OHDA rat model of Parkinson's disease. Cell Transplant. 21:749–762; 2012.
34. Richards, C. D.; Shiroyama, T.; Kitai, S. T. Electrophysiological and immunocytochemical characterization of GABA and dopamine neurons in the substantia nigra of the rat. Neuroscience 80:545–557; 1997.
35. Rohrbacher, J.; Ichinohe, N.; Kitai, S. T. Electrophysiological characteristics of substantia nigra neurons in organotypic cultures: Spontaneous and evoked activities. Neuroscience 97:703–714; 2000.
36. Rumpel, R.; Alam, M.; Klein, A.; Ozer, M.; Wesemann, M.; Jin, X.; Krauss, J. K.; Schwabe, K.; Ratzka, A.; Grothe, C. Neuronal firing activity and gene expression changes in the subthalamic nucleus after transplantation of dopamine neurons in hemiparkinsonian rats. Neurobiol. Dis. 59:230–243; 2013.
37. Rylander, D.; Bagetta, V.; Pendolino, V.; Zianni, E.; Grealish, S.; Gardoni, F.; Di Luca, M.; Calabresi, P.; Cenci, M. A.; Picconi, B. Region-specific restoration of striatal synaptic plasticity by dopamine grafts in experimental parkinsonism. Proc. Natl. Acad. Sci. USA 110:E4375–E4384; 2013.
38. Sawamoto, K.; Nakao, N.; Kobayashi, K.; Matsushita, N.; Takahashi, H.; Kakishita, K.; Yamamoto, A.; Yoshizaki, T.; Terashima, T.; Murakami, F.; Itakura, T.; Okano, H. Visualization, direct isolation, and transplantation of midbrain dopaminergic neurons. Proc. Natl. Acad. Sci. USA 98:6423–8; 2001.
39. Sørensen, A. T.; Thompson, L.; Kirik, D.; Björklund, A.; Lindvall, O.; Kokaia, M. Functional properties and synaptic integration of genetically labelled dopaminergic neurons in intrastriatal grafts. Eur. J. Neurosci. 21:2793–2799; 2005.
40. Tepper, J. M.; Trent, F.; Nakamura, S. Postnatal development of the electrical activity of rat nigrostriatal dopaminergic neurons. Dev. Brain Res. 54:21–33; 1990.
41. Timmer, M.; Grosskreutz, J.; Schlesinger, F.; Krampfl, K.; Wesemann, M.; Just, L.; Bufler, J.; Grothe, C. Dopaminergic

properties and function after grafting of attached neural precursor cultures. Neurobiol. Dis. 21:587–606; 2006.
42. Torres, E. M.; Lane, E. L.; Heuer, A.; Smith, G. A.; Murphy, E.; Dunnett, S. B. Increased efficacy of the 6-hydroxydopamine lesion of the median forebrain bundle in small rats, by modification of the stereotaxic coordinates. J. Neurosci. Methods 200:29–35; 2011.
43. van Horne, C. G.; Mahalik, T.; Hoffer, B.; Bygdeman, M.; Almqvist, P.; Stieg, P.; Seiger, A.; Olson, L.; Strömberg, I. Behavioral and electrophysiological correlates of human mesencephalic dopaminergic xenograft function in the rat striatum. Brain Res. Bull. 25:325–334; 1990.
44. Wahl-Schott, C.; Biel, M. HCN channels: Structure, cellular regulation and physiological function. Cell. Mol. Life Sci. 66:470–494; 2009.
45. Washio, H.; Takigachi-Hayashi, K.; Konishi, S. Early postnatal development of substantia nigra neurons in rat midbrain slices: Hyperpolarization-activated inward current and dopamine-activated current. Neurosci. Res. 34:91–101; 1999.
46. Winkler, C.; Kirik, D.; Björklund, A. Cell transplantation in Parkinson's disease: How can we make it work? Trends Neurosci. 28:86–92; 2005.
47. Zhang, T.; Placzek, A. N.; Dani, J. A. In vitro identification and electrophysiological characterization of dopamine neurons in the ventral tegmental area. Neuropharmacology 59:431–436; 2010.